

Zeitschrift: Schweizerische mineralogische und petrographische Mitteilungen = Bulletin suisse de minéralogie et pétrographie
Band: 73 (1993)
Heft: 2

Artikel: Regional metamorphism and uplift along the southern margin of the Gotthard massif : results from the Nufenenpass area
Autor: Kamber, Balz Samuel
DOI: <https://doi.org/10.5169/seals-55572>

Nutzungsbedingungen

Die ETH-Bibliothek ist die Anbieterin der digitalisierten Zeitschriften auf E-Periodica. Sie besitzt keine Urheberrechte an den Zeitschriften und ist nicht verantwortlich für deren Inhalte. Die Rechte liegen in der Regel bei den Herausgebern beziehungsweise den externen Rechteinhabern. Das Veröffentlichen von Bildern in Print- und Online-Publikationen sowie auf Social Media-Kanälen oder Webseiten ist nur mit vorheriger Genehmigung der Rechteinhaber erlaubt. [Mehr erfahren](#)

Conditions d'utilisation

L'ETH Library est le fournisseur des revues numérisées. Elle ne détient aucun droit d'auteur sur les revues et n'est pas responsable de leur contenu. En règle générale, les droits sont détenus par les éditeurs ou les détenteurs de droits externes. La reproduction d'images dans des publications imprimées ou en ligne ainsi que sur des canaux de médias sociaux ou des sites web n'est autorisée qu'avec l'accord préalable des détenteurs des droits. [En savoir plus](#)

Terms of use

The ETH Library is the provider of the digitised journals. It does not own any copyrights to the journals and is not responsible for their content. The rights usually lie with the publishers or the external rights holders. Publishing images in print and online publications, as well as on social media channels or websites, is only permitted with the prior consent of the rights holders. [Find out more](#)

Download PDF: 01.07.2025

ETH-Bibliothek Zürich, E-Periodica, <https://www.e-periodica.ch>

Regional metamorphism and uplift along the southern margin of the Gotthard massif; results from the Nufenenpass area

by Balz Samuel Kamber¹

Abstract

A new hypothesis for the strong N to S increase of metamorphic conditions in the Nufenenpass area was made possible by identifying the Cornoschuppe as a Penninic tectonic unit, possibly as a part of the sedimentary cover of the Lebendun crystalline nappe. Detailed lithological comparison between the Corno profile and the adjacent Ultrahelvetetic Nufenenzone showed rocks typical for the Northpenninic realm, such as Permo-Carboniferous psammitic gneisses, much higher abundance and variety of Triassic marbles as well as conspicuous garnet-quartz-plagioclase-felses. The lithological evidence is supported by microstructural observations of chemically similar strata mainly showing that garnet porphyroblasts grew post-deformational in the Lias of Nufenenzone but are strongly rotated in corresponding Corno rocks. A metamorphic profile from the Gotthard massif into the Penninic Bündnerschiefer is fully consistent with this interpretation. Rocks N from the newly defined Helvetic-Penninic tectonic boundary hold peak-conditions grouped between 465 to 490 °C and 4800 to 5000 bar whereas the Penninic rocks hold 515–525 °C around 6000 bar. The abrupt increase of metamorphic conditions on one hand underscores petrographic and microstructural observations and on the other hand documents syn- to post-peak metamorphic motion along the Helvetic-Penninic boundary, lifting the southern units with respect to the northern ones. This locus of major movement is characterized by a striking abundance of hornblende-garbenschiefer in its close vicinity. Mineral growth-deformation relations show that hornblende is a syn- to post-D3 porphyroblast. These rocks interestingly hold the same peak-P-T conditions as do the Penninic rocks in the area which poses new questions about timing and locus of the climax of Tertiary metamorphism in the northern Lepontine Alps. Clearly the strong increase of metamorphic conditions in the Nufenenpass area is due to juxtaposition of higher- and lower grade rocks. There is no evidence for an anomalously high geothermal gradient which has formerly been used to explain the metamorphic pattern. Observed growth deformation relations as well as the metamorphic profile can be explained in terms of syn- to post-peak vertical block movement (RIDLEY, 1989). Further studies along the southern border of the Gotthard massif, e.g. in Val Piora, will show whether the model of major syn- to post-D3 motion can be applied in an extended regional scale.

Keywords: hornblende-garbenschiefer, metamorphic climax, uplift, Helvetic-Penninic boundary, Gotthard massif, Central Alps.

Introduction

The Nufenenpass area has been the site of many geological studies. It offers a well-exposed profile from the Gotthard massif through its Helvetic cover into the somewhat "exotic" Cornoschuppe – first described by OBERHOLZER (1955) – and the northernmost pile of Penninic Bündnerschiefer. Subdivisions of the Gotthard massif by HAFNER (1958), its Helvetic cover called the Nufenen zone (EICHENBERGER, 1924) and the Penninic Bündner-

schiefer locally called the Bedrettozone (PROBST, 1980) have been established for some time and are generally accepted. In contrast, the very existence of the Cornoschuppe is contested. After the definition of this structural unit (OBERHOLZER, 1955), most subsequent authors (LISZKAY, 1966; HANSEN, 1972 or KLAPER and BUCHER-NURMINEN, 1987) have included it in the Helvetic Nufenenzone, whereas LEU (1985) raised the possibility that at least parts of the Cornoschuppe could represent Penninic-facies rocks belonging to the

¹ Mineralogisch-petrographisches Institut, Universität Bern, Erlachstr. 9A, CH-3012 Bern, Switzerland.

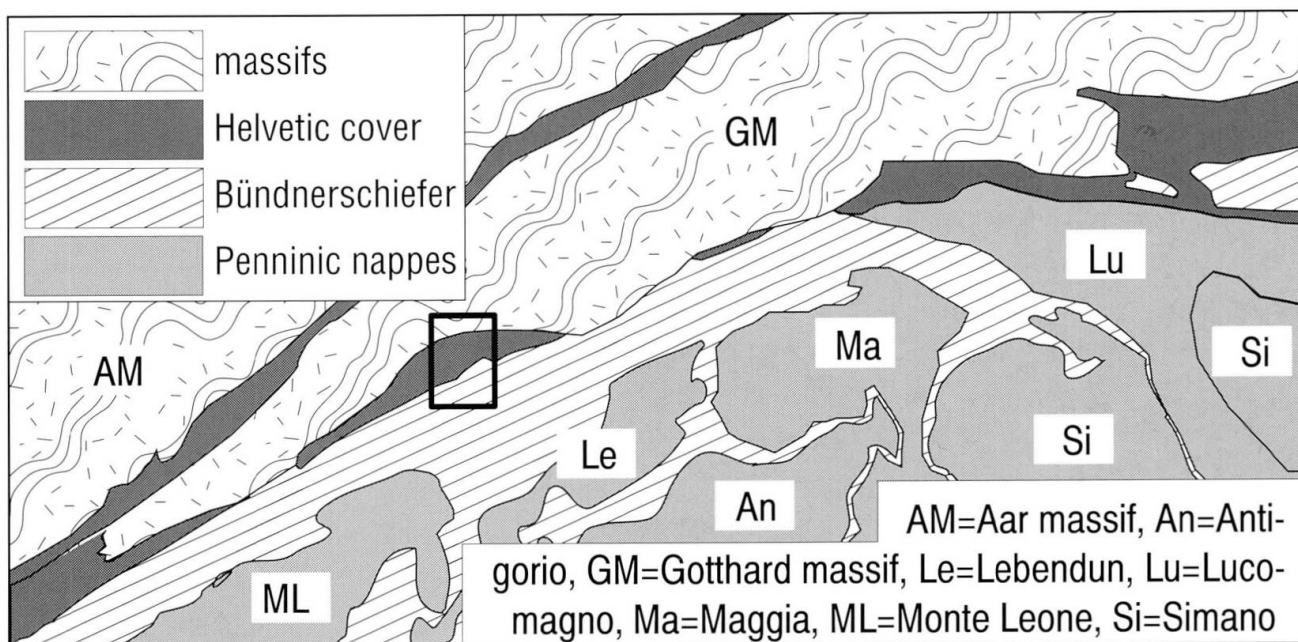


Fig. 1 Tectonic sketch map of the Central Swiss Alps. The study area is outlined.

sedimentary cover of the Lebendun crystalline. This means that LEU (1985) shifted the Helvetic-Penninic tectonic boundary to the north. Condensed isogrades, possibly steep dipping (FOX, 1975), along the southern border of the Gotthard massif (e.g. KLAPER and BUCHER-NURMINEN, 1987) could be the result of a back folding event and/or relative movement along subvertical structures. In trying to evaluate which processes played an important role to form the northern steep belt (MILNES, 1974) the exact location of the border between Helvetic and Penninic tectonic units is of some importance.

This paper deals specifically with the Helvetic-Penninic tectonic boundary zone. Lithostratigraphic and structural studies are used to define the exact location between Helvetic and Penninic tectonic units. Determinations of P-T conditions using the internally consistent data set of BERMAN (1988) are used to verify the importance of the Cornoschuppe and to gain for further insight into the complex Alpine history along the southern border of Gotthard massif.

Geological framework

The study area is located at the south-western end of the Gotthard massif between Nufenenpass and Griespass (Swiss-Italian border) as illustrated on figure 1. The following four units may be distinguished within it (Fig. 2):

GOTTHARD MASSIF

The northern part of the study area belongs to the "mittlere Gneiszone" of the Gotthard massif as defined by HAFNER (1958). The main rock types are two-mica paragneisses, which may be garnetiferous and/or clinozoisite bearing, an inlayer of orthogneiss (a characteristic Kfs² augengneiss) plus some minor lenses of garnet amphibolites. Like elsewhere in the Gotthard massif, unraveling of at least Alpine and Variscan, and perhaps an even earlier history, is not simple. Without information on the age of magmatic and metamorphic minerals, only limits can be set (e.g. ABRECHT et al., 1991).

NUFENENZONE

The parautochthonous Mesozoic sedimentary cover of the Gotthard massif ranges from Triassic rauhwaacke, pure dolomitic marble and Quaternary schiefer (mostly chlorite bearing micaceous schists) to Liassic garnetiferous graphite-bearing micaschists, quartzites and calcareous clinozoisite- or plagioclase-porphyroblast bearing schists. It forms a giant isoclinal fold to imbricate type edifice resulting from isoclinal folding. The axial planes of these isoclinal folds have a very con-

² Mineral abbreviations following KRETZ (1983).

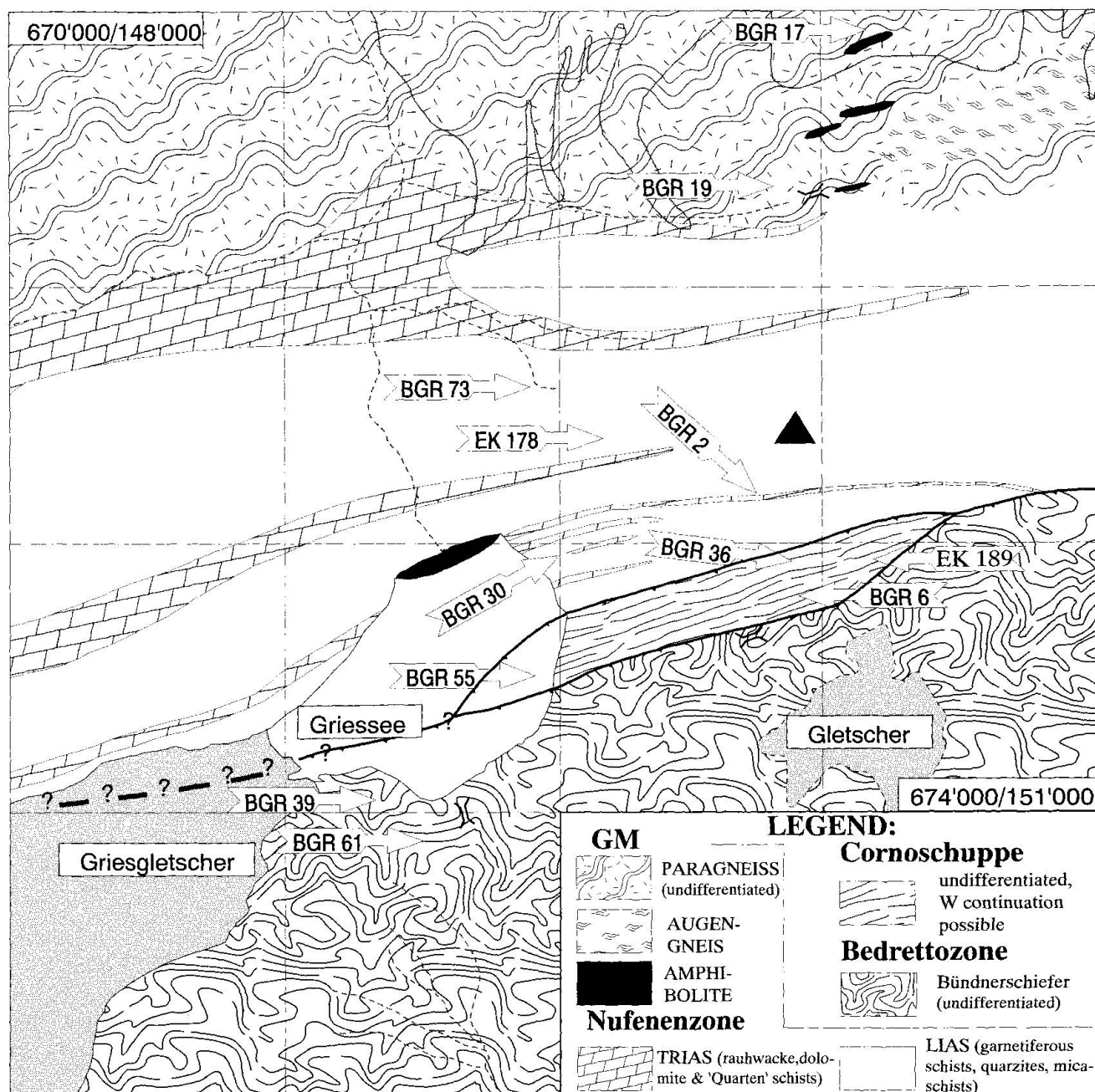


Fig. 2 Geological sketch map of the study area. Arrows indicate sample localities which are used for the N-S metamorphic profile along coordinate 672'000.

stant, N88°E, strike, but the fold axes dip very variably from 17°E to 72°W, typical for a sheath-fold style. The overall structural pattern and the mineralogy of the different strata are very homogeneous in the northern three of four folds, whereas the southernmost fold features some differences. Although it is somewhat poorly exposed, detailed mapping of this foldlimb suggests an internal small scale imbricate structure. Besides the structural difference, there is also a bigger variety of metamorphic minerals including the

first occurrence of *garben* textured hornblende – as already noted by OBERHOLZER (1955) – in most strata and garnet as well as paragonite in the *Quarten* series.

CORNOSCHUPPE

The dramatic retreat of the Gries glacier in the second half of this century has allowed more detailed mapping of this unit, which was previously

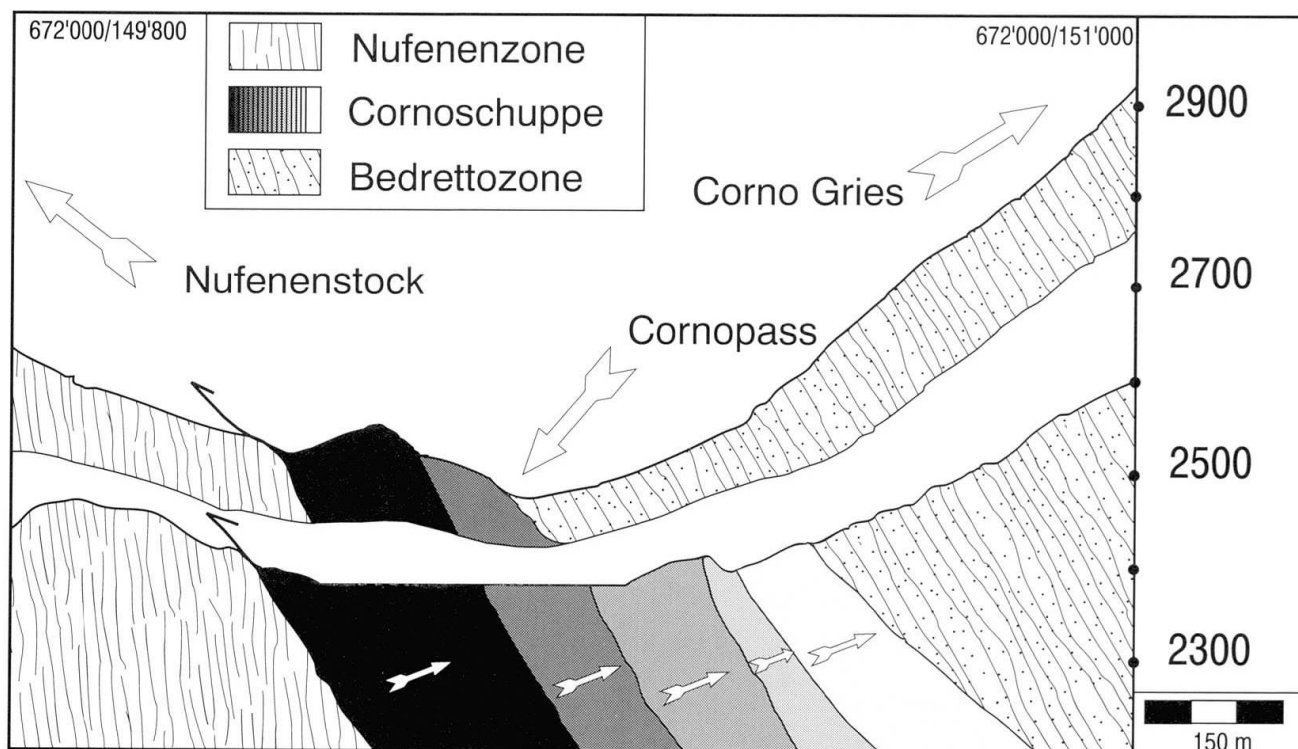


Fig. 3 Sketch profile through the Cornoschuppe looking east. Polarities of the five imbricates are indicated by arrows and were constructed from detailed mapping along lake Gries (in front) and from patchy outcrops further east at the Cornopass (behind).

covered by ice and moraine. The internal structure reconstructed from the patchy outcrops and a profile taken along the edge of Lake Gries can be described as a set of five south dipping ($\approx 35^\circ$) imbricates. Each of these only spans a part of the whole stratigraphy beginning with Permo-Carboniferous conglomerate to psammitic gneisses at the base, followed by Triassic arkose, rauhwacke, marbles (much thicker than in the Nufenen zone stratigraphy) and Quartenschiefer with Liassic garnetiferous, graphite-bearing micaschists at the top. Important lithological and structural differences between this unit and the Nufenenzone will be treated in detail in the next section.

BEDRETTOZONE

The Penninic Bündnerschiefer, mostly undifferentiated Liassic (PROBST, 1980) calcareous micaschists, build up an enormous stack which dominates the landscape as a chain with some impressive peaks (e.g. Griesstock). Only at the base of the series can some Triassic rocks, mainly rauhwacke and some outcrops of Quartenschiefer, be detected. While structures are very well developed, not much petrologic and stratigraphic information can be gained. We simply miss inter-

esting metamorphic minerals suitable for P-T determinations in these monotonous calcareous micaschists. Complex fold interference patterns are the result of strong compression during late D2 and D3 in the concept of KLAPER (1986) obliterating most of the former D2 structures, which are predominant in the Helvetic Nufenenzone.

The Helvetic-Penninic boundary

One goal of this paper is to define the exact location of the Helvetic-Penninic tectonic boundary and to focus on some of its characteristics, which could help to improve our understanding of the tectono-metamorphic history of the southern border of the Gotthard massif. Detailed mapping and observation of lithologies showed differences between the Nufenenzone and the Cornoschuppe. Correlation with other metasedimentary covers lead to the working hypothesis that the Cornoschuppe might be a part of a Penninic sedimentary cover, maybe of the Lebendun crystalline nappe. Microstructural observations and a detailed metamorphic profile support this hypothesis. Even though the actual contact between the Helvetic Nufenen zone and the possibly Penninic Cornoschuppe cannot be observed directly

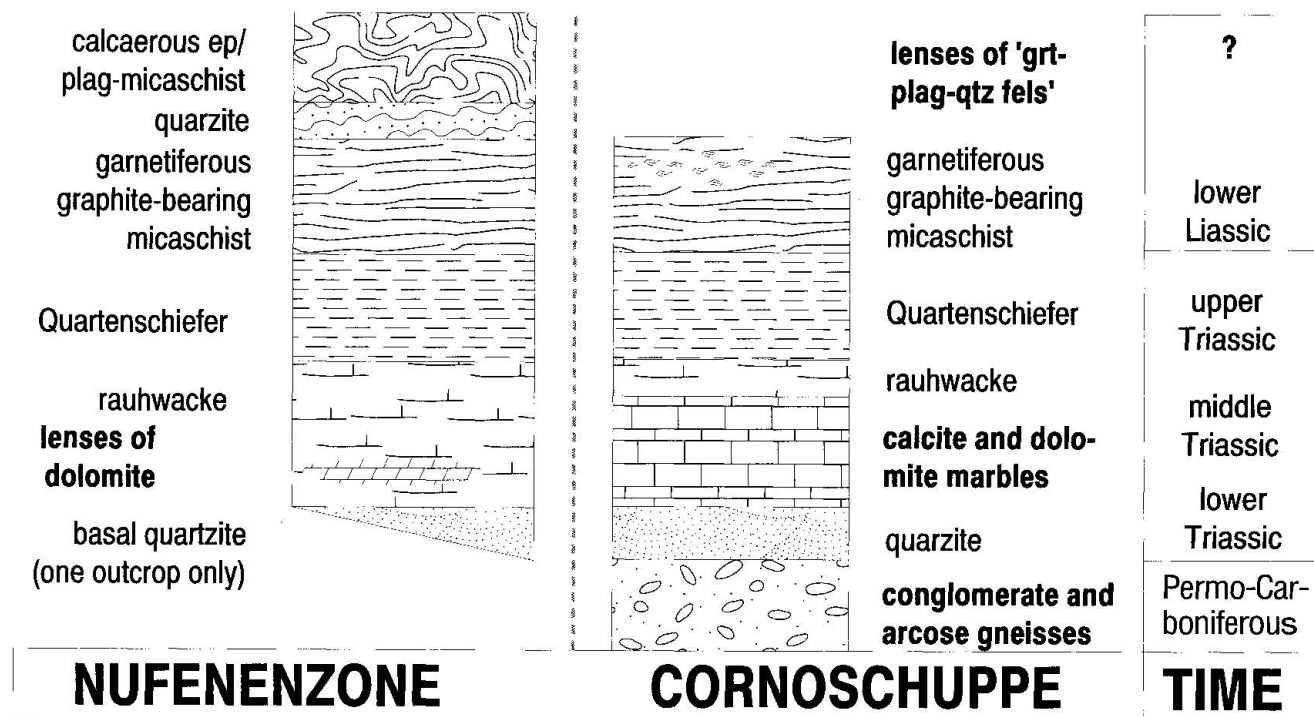


Fig. 4 Comparison of schematic lithological profiles of Nufenenzone (Ultrahelvetic realm) and Cornoschuppe (North-penninic realm). Important differences are marked by arrows and discussed in the text.

in the field, petrologic work does confirm its late tectonic character and emphasizes its significance in the Cornopass area.

LITHOSTRATIGRAPHIC CHARACTERIZATION OF THE CORNOSCHUPPE

The Mesozoic sedimentation in the Ultrahelvetic domain (e.g. the Nufenenzone) is very similar to that of the adjacent North-penninic realm (e.g. the cover of Lebendun crystalline). Together with the fact that most of the Cornoschuppe is still covered by moraine, this has led to substantial confusion about the palinspastic position of this unit (for a detailed outline see LEU, 1985). OBERHOLZER (1955), who was the first to find leucocratic gneisses and biotite granite within the Cornoschuppe, identified it as a distinct structural unit. Because of the similarity of the biotite granite with the Rotondo granite and of most of the Mesozoic metasediments with those of the Nufenenzone he believed the Cornoschuppe to be a slice of the Gotthard massif with its cover, juxtaposed onto the "normal" southern border of the Gotthard massif. LEU (1985) found the Cornoschuppe to consist of five slightly south-dipping imbricates, contrasting OBERHOLZER's (1955) interpretation as an anticline with crystalline

Gotthard massif rocks in its core. One of these imbricates with leucocratic gneiss at its base and a great abundance of "exotic" marbles – compared with the Nufenen zone stratigraphy – was assigned to the sedimentary cover of the Lebendun crystalline.

Detailed mapping and a profile taken along the edge of Lake Gries allowed to distinguish five imbricates, all of them with N to S stratigraphic polarity as illustrated on figure 3. All of these imbricates contain at least one lithostratigraphic element which does not fit the Nufenenzone stratigraphy. A detailed comparison between the Nufenenzone and the Cornoschuppe stratigraphies shows three main differences (compare with Fig. 4):

(i) The base of the Lebendun pile is formed of Permo-Carboniferous conglomerate to psammite gneisses. The chemical comparison of a psammitic gneiss from the Cornoschuppe (BGR50) with a typical metapelite gneiss from the Simplon area (J373'e of Joos, 1969) in table 1 shows good agreement in all major elements. One single outcrop of basal quartzite in the whole Nufenen area might correspond to the Triassic quartzites of the Lebendun pile. Otherwise there is no evidence for basal clastic metasediments in this part of the Gotthard massif cover.

(ii) Whereas marbles in the Nufenenzone are

Tab. 1 Main elements by XRF method.

sample	J373'e	BGR 50	BGR 73	BGR 69
SiO ₂	78.10	80.90	57.86	56.51
TiO ₂	0.20	0.12	1.07	0.78
Al ₂ O ₃	12.30	10.10	19.24	18.03
Fe ^{tot}	1.00	0.20	7.96	6.97
MnO	0.02	0.01	0.13	0.02
MgO	0.50	0.19	2.10	6.39
CaO	0.60	0.10	5.53	5.15
Na ₂ O	2.50	1.80	1.14	1.27
K ₂ O	4.10	4.20	2.51	2.31
P ₂ O ₅	0.00	0.02	0.11	0.09
LOI	0.70	0.70	2.03	2.68
Total	100.2	98.30	99.68	100.19

confined to thin slivers within *rauhwacke*, they are the thickest Triassic strata in the Corno sediments (except for the northernmost imbricate with the dominant *rauhwacke* range). Not only are they thicker but they also show greater mineralogical variety (cal, grt, chl, pg, czo, kfs) compared to the pure dolomitic ones from the Nufenen zone.

(iii) Joos (1969) describes lenses of "grt-qtz-pl"-fels distinctive of the Liassic garnetiferous graphite bearing micaschists of the Lebendun stratigraphy. Although very well exposed in the Nufenenzone, Liassic strata lack this very conspicuous rock type, whereas even the untrained eye can find it in the poorly exposed Cornoschuppe.

The fact that every imbricate of Cornoschuppe features one or more of the above mentioned characteristics led to the idea that the Cornoschuppe might represent a part of the cover of the Lebendun crystalline. This idea is in contrast to the interpretation of LEU (1985) who, based on the recognition of anticlinal structures, divided the five imbricates into true Gotthard massif cover and Lebendun sedimentary cover. However, the possibility that the entire Cornoschuppe might belong to the Lebendun sedimentary cover will be kept in mind when interpreting structural and petrologic results.

STRUCTURAL DIFFERENCES BETWEEN NUFENENZONE AND CORNOSCHUPPE

The deformational history of the area has been well investigated (e.g. RAMSAY, 1979; KLAPER, 1986). The mega- to mesoscale concept of KLAPER (1986) will be used here to examine whether dif-

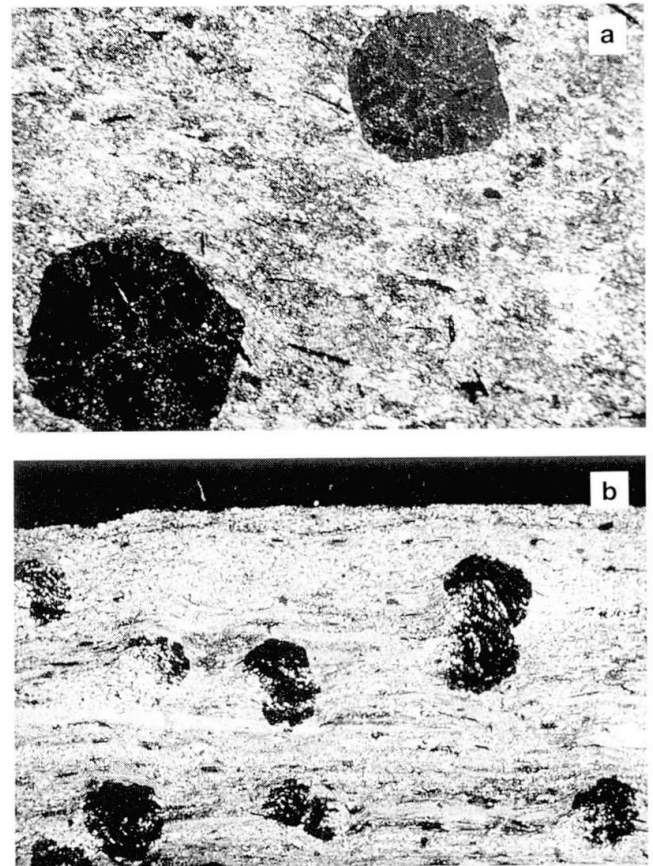


Fig. 5 Microphotographs of graphitic Liassic garnetiferous schists similar in chemistry (see also Tab. 1). Picture a) is taken from Nufenenzone and shows undeformed grt porphyroblasts with radially arranged solid inclusions (mainly qtz and tur). These porphyroblasts are interpreted to have grown post-deformational because they grew over the schistosity (S2). Picture b) is from the Cornoschuppe and shows the same mineralogy as the first. These grt porphyroblasts are strongly deformed, matrix minerals "swim" around them, inclusions are S-shaped and indicate rotation. These porphyroblasts are interpreted to have grown syn-deformational growing over a S2 schistosity which starts to be crenulated by D3. Size of big grt porphyroblasts is 8 mm.

ferences between the Helvetic Nufenenzone and the possibly Penninic Cornoschuppe can be documented. Following this concept the deformation can be split into three distinct steps D1, D2 and D3:

(D1) This phase is responsible for the establishment of the different nappes and for the first folding of these.

(D2) During this step open D1 folds are compressed to isoclinal ones, coinciding with the formation of a strong foliation, generally parallel to one of the fold limbs but penetrating the other at a low angle. Further non-coaxial folding of isoclinal folds is restricted to Penninic rocks.

(D3) The last fold producing event, contemporaneous with the formation of the northern steep belt (MILNES, 1974) is documented by chevron type small scale folding. In the Nufenenzone only very mica rich rocks developed a crenulation.

According to this concept, Penninic rocks could possibly be distinguished from Helvetic ones by differences in structure. The question was, whether the metasediments from the Cornoschuppe feature structures characteristic for Penninic rocks – mainly complex fold interference patterns and strong crenulation even in less mica rich rocks – or not. There are differences between structures in the Nufenenzone and the Cornoschuppe. This concerns the structures related to D3 which are much better evolved in the Cornoschuppe. Still there is no compelling mega- to meso-scale structural evidence in the the Cornoschuppe, for assigning it either to the Helvetic or to the Penninic.

In contrast, microstructures, essentially mineral growth-deformation relations, show clear differences. Photographs of Liassic garnetiferous graphite bearing micaschists from the Nufenenzone and the Cornoschuppe – which, except for Mg, are chemically very similar (see BGR73 and BGR 69 in Tab. 1) – are shown in figure 5. The difference is striking; garnets from the Nufenenzone do not show any sign of post-growth deformation, whereas the ones from the Cornoschuppe are strongly rotated. Although less distinctive this is also true for plagioclase porphyroblasts in the Quartenschiefer. The fact, that in chemically similar rocks, garnets grew at different times relative to deformation, means that both rocks underwent different P-T-deformation histories.

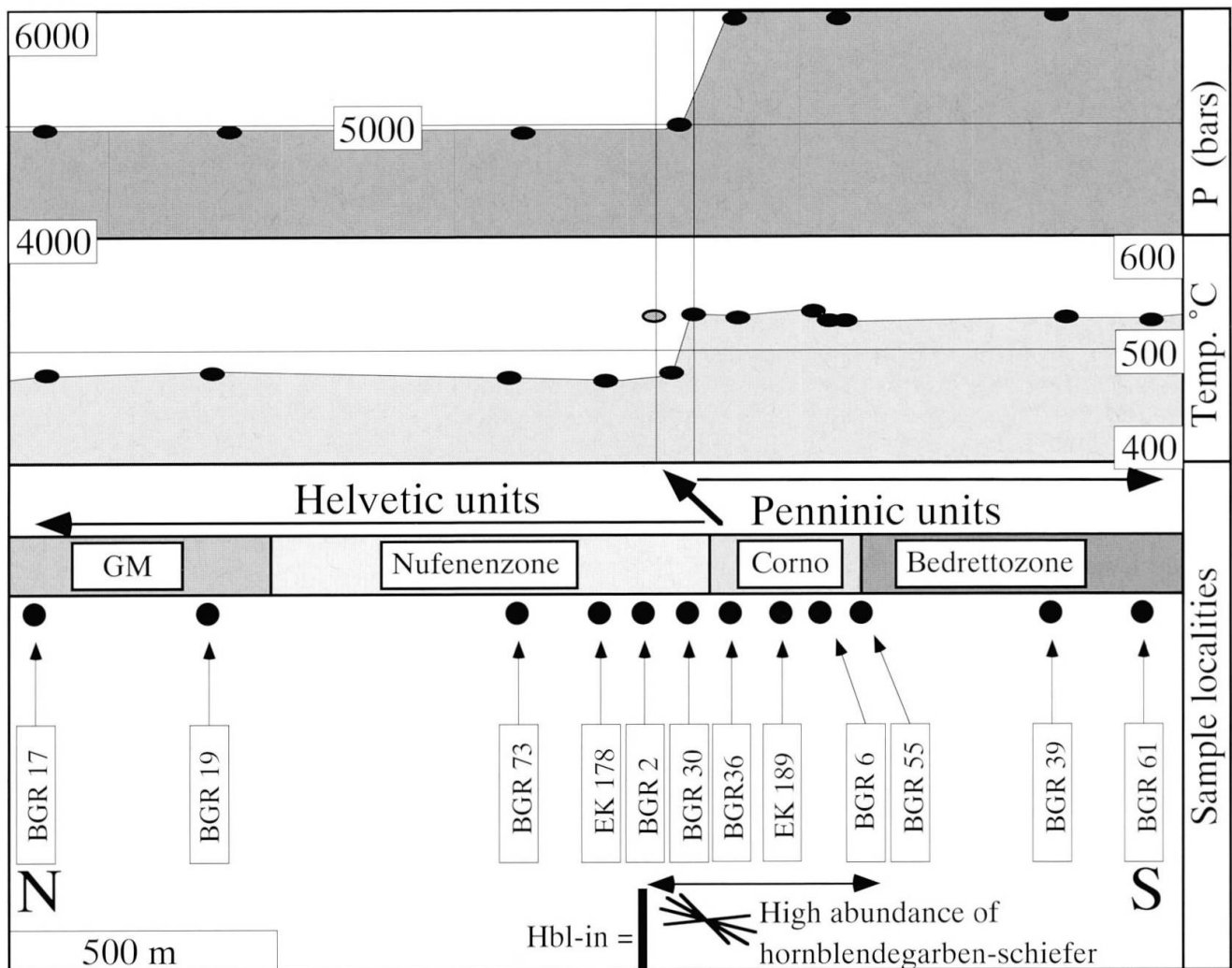


Fig. 6 Metamorphic profile constructed from samples listed in table 2 and localized on figure 2, projected onto coordinate 672'000. T and P (if estimated) for each sample plotted versus distance. This shows the abrupt increase in P and T along the contact between Nufenenzone and Cornoschuppe. T increases already within the southernmost Nufenenzone. This is due to the fact that BGR 2 is a hornblende-garben-schiefer which indicates the same T as the Penninic rocks. It can also be seen that the increase in P is less well defined because suitable barometric reactions cannot be found in all the different lithologies.

The important aspect of this observation is, that the variation in timing of porphyroblast growth as well as the increase of D3 related microstructures towards the south are not continuous over the profile, but bound to the Nufenenzone-Cornoschuppe contact. On one hand this constitutes further evidence for the theory that the Cornoschuppe is not just a fifth imbricate of the Nufenenzone. On the other hand this corresponds with the predictions of RIDLEY'S (1989) subvertical block movement model. Upthrowing of the southern Penninic block relative to the northern Helvetic block during D3 limits porphyroblast growth to pre- to syndeformational in the south due to cooling whereas porphyroblasts in the northern downthrown block preferentially form upon heating during or after peak-D3 deformation.

Alpine metamorphism

An attempt was made to obtain a P-T profile ranging from the Gotthard massif into the Bedrettozone, in order to get information concerning the timing of juxtaposition of the different units relative to metamorphism. The lithostratigraphic diversity of the Mesozoic metasediments offers a choice of suitable candidates for P-T estimations in all the tectonic units, except for the Gotthard massif. The problem with the garnetiferous czo-bearing micagneisses from the Gotthard massif lies in the possibility of P-T results corresponding to a pre-Alpine metamorphism. Samples were selected on the basis of suitable mineralogy and homogenous distribution along the N-S profile. Where recalculation from published mineral chemistry was possible, data points (labelled EK) from KLAPER and BUCHER-NURMINEN (1987) were included. A short petrographic description of each sample is given in the Appendix.

The resulting N-S metamorphic profile, constructed from 12 P-T estimations, is presented in figure 6. An outline on how these estimations were deduced, as well as a discussion, are given in the following sections.

DETERMINATION OF PEAK P-T CONDITIONS

Estimation of metamorphic equilibrium P-T, $T-X_{\text{CO}_2}$ or $P-X_{\text{CO}_2}$ conditions by means of equilibria diagrams calculated on the basis of an internally consistent thermodynamic database (including consistent activity-composition models and equations of state) yields advantages over the use of single thermo-barometers (e.g. LIEBERMAN and

PETRAKAKIS, 1991). Applying this approach to a metamorphic profile makes good use of these advantages:

i) In a metamorphic profile we are primarily interested in the variation of P-T, $T-X_{\text{CO}_2}$ or $P-X_{\text{CO}_2}$ conditions from one point to another. The internally consistent database ensures that no artificial ΔP -T is calculated as it can happen when using inconsistent calibrations for different thermo-barometers from the literature.

ii) As long as we are only interested in ΔP -T between different points of the profile and not in absolute P-T values, the errors in the calculated conditions are only due to imprecisions in electron microprobe data.

iii) Equilibrium diagrams can be a measure of the validity of the microscopically determined paragenesis and the preservation of equilibrium in the sample visualized by the distribution of mutual P-T intersections among the equilibria. This seems to be a very important advantage, as single grt-bio thermometry for example will not tell whether bio was ever in equilibrium with grt (e.g. late "Quer"-biotite).

The metamorphic N-S profile presented in this work has been done with equilibrium diagrams calculated using PTAX, a further development of GEOCALC (BERMAN et al., 1987), with the internally consistent data set of BERMAN (1988) supplemented with consistent thermodynamic properties for tschermakite from experimental and empirical constraints (LIEBERMAN and KAMBER, 1991). Activity models used comprise FUHRMAN and LINDSLEY (1988) for plagioclase, EUGSTER et al. (1972) for white mica, BERMAN (1990) for garnet, INDARES and MARTIGNOLE (1985) for biotite, KOHN and SPEAR (1990) for hornblende and KERRICK and JACOBS (1981) for H_2O , CO_2 and mixtures. For all other phases (clz, cld and chl) simple ideal site solution was assumed.

Every phase that makes part of a paragenesis, as determined from the microscopic growth-deformation relations, has been analysed with the electron microprobe. Mineral chemistries (except for nearly pure phases like qtz, cal and dol) are presented in table 3.

Due to the limited number of available thermodynamic endmember data and because of $a_{\text{H}_2\text{O}}$ -dependent equilibria, it was not always possible to construct sensible P-T diagrams. $T-X_{\text{CO}_2}$ diagrams at a reasonably fixed P (BGR36, 39, 61) and ms-pg solvus thermometry (BGR30) had to be used instead.

All the P-T, $T-X_{\text{CO}_2}$, and T-X ms (BGR30) diagrams are shown on figure 7. Each of these diagrams (except for the ms-pg solvus thermometer

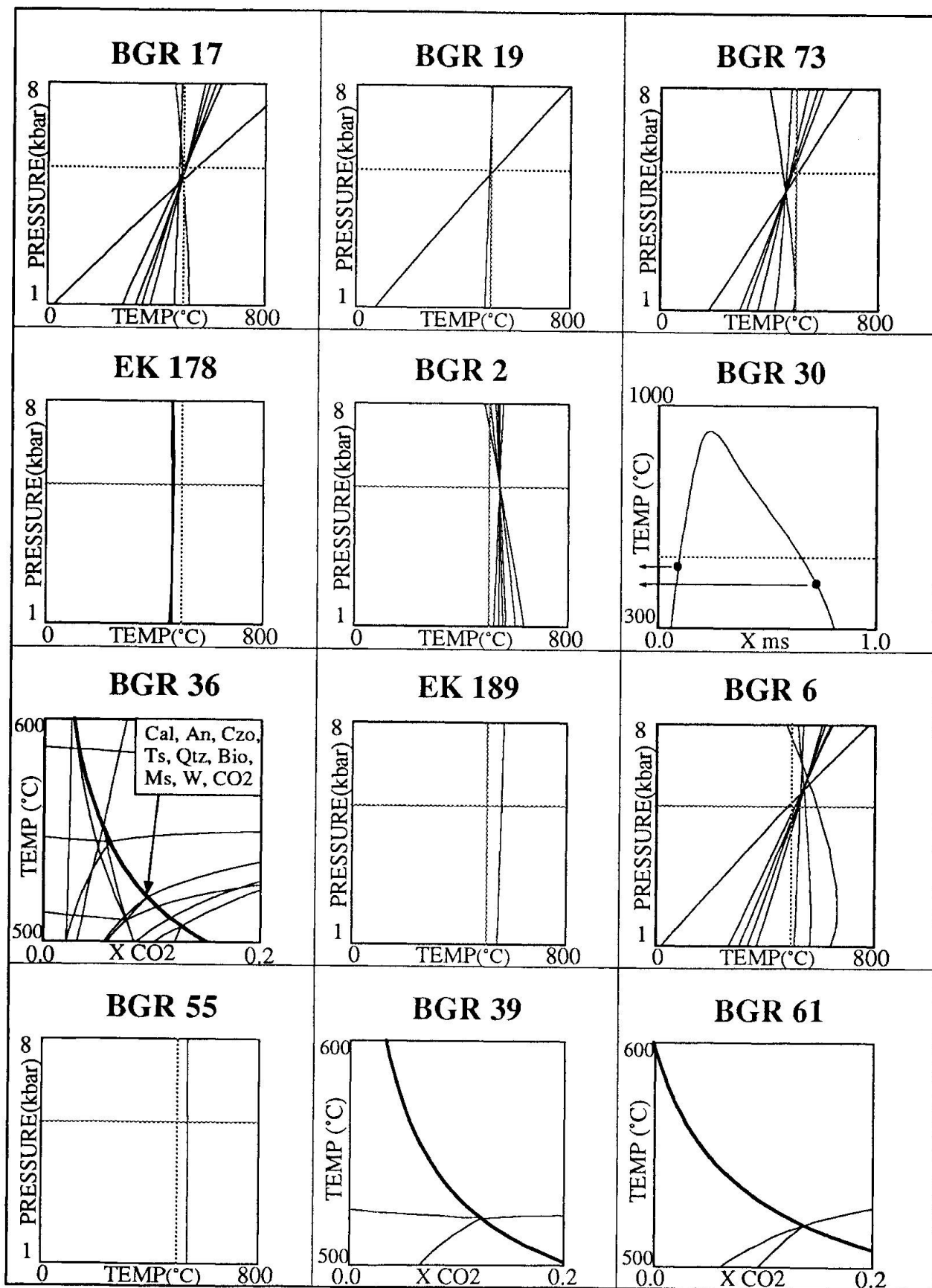


Fig. 7 Compilation of all the P-T, T-X_{CO₂} and T-X ms equilibrium diagrams used to estimate metamorphic peak-conditions. Dotted crosses at 500 °C and 5 kbar plotted for reference. Information on chemical systems, reactants, reactions, fixed a_{H_2O} and fixed P respectively can be seen from table 2.

Tab. 2 Parageneses, reactions and P-T-X_{CO₂} estimations used for the metamorphic profile (Fig. 7).

Sample No 1) Paragenesis 2) Chemical system 3) Endmembers	Reactions (at fixed P, T or a H ₂ O)	P and/or T estimated
BGR17 1) grt-qtz-pl-bio-ms-clz-W 2) K-Ca-Fe-Mg-Al-Si-O-H 3) qtz-an-phl-ann-clz-ms-grs-py-alm-W	$4 \text{ Clz} + \text{aQz} = 5 \text{ An} + \text{Gr} + 2 \text{ W}$ (a H ₂ O = 1) $4 \text{ Clz} + \text{aQz} + \text{Ms} + \text{Alm} = \text{Ann} + 8 \text{ An} + 2 \text{ W}$ $\text{Phl} + \text{Alm} = \text{Ann} + \text{Py}$ $\text{Alm} + \text{Gr} + \text{Ms} = 3 \text{ An} + \text{Ann}$ $4 \text{ Clz} + \text{aQz} + \text{Py} + \text{Ms} = 8 \text{ An} + \text{Phl} + 2 \text{ W}$ $\text{Py} + \text{Ms} + \text{Gr} = 3 \text{ An} + \text{Phl}$ $6 \text{ W} + 5 \text{ Py} + 5 \text{ Ms} + 8 \text{ Gr} = 5 \text{ Phl} + 3 \text{ aQz} + 12 \text{ Clz}$	480°C/4.8kbar
BGR19 1) qtz-pl-bio-ms-W 2) K-Ca-Fe-Mg-Al-Si-O-H 3) qtz-an-phl-ann-ms-grs-py-alm-W	$\text{Phl} + \text{Alm} = \text{Ann} + \text{Py}$ (a H ₂ O = 1) $\text{Py} + \text{Ms} + \text{Gr} = 3 \text{ An} + \text{Phl}$ <i>irrelevant for these reactions</i>	490°C/4.9kbar
BGR 73 same as BGR17	same as BGR17 (a H ₂ O = 1)	465°C/4.7kbar
EK178 1) cld-grt-qtz-chl-W 2) Ca-Fe-Mg-Al-Si-O-H 3) Fcld-py-alm-dph-cln-qtz-W	$\text{Fclcd} + \text{Dph} + 2 \text{ Qtz} = 5 \text{ W} + 2 \text{ Alm}$ (a H ₂ O = 1) $3 \text{ Fclcd} + 3 \text{ Cln} + 6 \text{ Qtz} = 15 \text{ W} + 5 \text{ Py} + \text{Alm}$ $3 \text{ Dph} + 5 \text{ Py} = 3 \text{ Cln} + 5 \text{ Alm}$ $5 \text{ Fclcd} + 6 \text{ Cln} + 10 \text{ Qtz} = 25 \text{ W} + 10 \text{ Py} + \text{Dph}$	470 to 480°C between 2 and 8 kbar
BGR2 1) qtz-pl-grt-bio-hbl-clz-ms-W 2) K-Ca-Fe-Mg-Al-Si-O-H 3) py-alm-grs-qtz-an-ann-phl-Mts-clz-ms-W	(a H ₂ O = 1) 530°C/5.0kbar $24 \text{ W} + 33 \text{ Qtz} + 20 \text{ Py} + 22 \text{ Gr} = 15 \text{ Ts} + 18 \text{ Clz}$ $18 \text{ W} + 4 \text{ Py} + 11 \text{ Ms} + 22 \text{ Gr} + 11 \text{ Alm} = 11 \text{ Ann} + 3 \text{ Ts} + 30 \text{ Clz}$ $6 \text{ W} + 5 \text{ Ms} + 8 \text{ Gr} + 5 \text{ Alm} = 5 \text{ Ann} + 3 \text{ Qtz} + 12 \text{ Clz}$ $3 \text{ Ann} + 4 \text{ Gr} + 8 \text{ Py} + 15 \text{ Qtz} + 6 \text{ W} = 6 \text{ Ts} + 3 \text{ Ms} + 3 \text{ Alm}$ $3 \text{ Ts} + 4 \text{ Ms} + 2 \text{ Gr} + 4 \text{ Alm} = 4 \text{ Ann} + 4 \text{ Py} + 9 \text{ Qtz} + 6 \text{ Clz}$ $11 \text{ Ann} + 16 \text{ Py} + 33 \text{ Qtz} + 12 \text{ Clz} + 6 \text{ W} = 12 \text{ Ts} + 11 \text{ Ms} + 11 \text{ Alm}$	
BGR30 1) qtz-pl-grt-ms pg-clz--W 2) K-Na-Al-Si-O-H 3) pg-ms	(P = 5 kbar) Paragonite-muscovite solvus thermometer was preferred because equilibrium diagram depends very strongly on a H ₂ O. For this rock the calibration of CHATTERJEE and FLUX (1986) was used.	minimum T 480°C
BGR36 1) qtz-cal-dol-pl-hbl-clz-ms-bio-(chl?)-W-CO ₂ 2) K-Ca-Mg-Al-Si-O-H-C 3) qtz-an-dol-cal-ann-phl-Mts-clz-ms-W <i>note: only reactions without chlorite are listed, because the diagram points to retrograde formation</i>	(P = 6 kbar) $3 \text{ An} + \text{Cal} + \text{W} = \text{CO}_2 + 2 \text{ Clz}$ $3 \text{ Cal} + \text{Ts} + 5 \text{ CO}_2 = \text{W} + 5 \text{ aQz} + 4 \text{ Dol} + \text{An}$ $\text{Ts} + 6 \text{ Clz} + 8 \text{ CO}_2 = 4 \text{ W} + 5 \text{ aQz} + 4 \text{ Dol} + 10 \text{ An}$ $10 \text{ Cal} + 3 \text{ Ts} + 14 \text{ CO}_2 = 2 \text{ W} + 2 \text{ Clz} + 15 \text{ aQz} + 12 \text{ Dol}$ $4 \text{ W} + 7 \text{ aQz} + 4 \text{ Phl} + 10 \text{ An} = 4 \text{ Ms} + 3 \text{ Ts} + 2 \text{ Clz}$ $14 \text{ CO}_2 + 8 \text{ Clz} + 5 \text{ Phl} = 5 \text{ An} + 7 \text{ Dol} + 5 \text{ Ms} + 2 \text{ Ts} + 2 \text{ W}$ $2 \text{ W} + 10 \text{ CO}_2 + 14 \text{ Clz} + 21 \text{ Qz} + 12 \text{ Phl} = 10 \text{ Cal} + 12 \text{ Ms} + 9 \text{ Ts}$ $37 \text{ CO}_2 + 14 \text{ Clz} + 15 \text{ Phl} + 5 \text{ Cal} = 21 \text{ Dol} + 15 \text{ Ms} + 6 \text{ Ts} + \text{W}$ $5 \text{ Cal} + \text{Phl} + \text{Ts} + 9 \text{ CO}_2 = \text{W} + 7 \text{ aQz} + \text{Ms} + 7 \text{ Dol}$ $3 \text{ W} + \text{CO}_2 + 7 \text{ aQz} + 4 \text{ Phl} + 7 \text{ An} = \text{Cal} + 4 \text{ Ms} + 3 \text{ Ts}$ $2 \text{ W} + 10 \text{ CO}_2 + 5 \text{ Phl} + 4 \text{ Cal} + 7 \text{ An} = 7 \text{ Dol} + 5 \text{ Ms} + 2 \text{ Ts}$	520°C/0.1 xCO ₂

Tab. 2 (continued)

Sample No 1) Paragenesis 2) Chemical system 3) Endmembers	Reactions (at fixed P, T or a H ₂ O)	T and/or P estimated
EK189 1) grt-bio 2) K-Fe-Mg-Al-Si-O-H 3) alm-ann-phl-py	Phl + Alm = Ann + Py (a H ₂ O = 1) <i>irrelevant for this reaction</i>	520 to 530°C between 2 and 8 kbar
BGR 6 same as BGR17 <i>P estimate for BGR6 is taken to be relevant so that T-XCO₂ diagrams are based on 6.0kbar.</i>	same as BGR17 (a H ₂ O = 1)	515°C/6.1kbar
BGR55 1) grt-chl-dol-qtz-clz 2) Fe-Mg-Ca-Al-Si-O-H 3) alm-cln-daph-py	Cln + Alm = Daph + Py (a H ₂ O = 1) <i>irrelevant for this reaction</i>	520 to 525°C between 2 and 8 kbar
BGR39 1) qtz-cal-pl-hbl-clz-ms-bio-W-CO ₂ 2) K-Ca-Mg-Al-Si-O-H-C 3) qtz-an-cal-phl-Mts-clz-ms-W-CO ₂	(P = 6kbar) 3 An + Cal + W = CO ₂ + 2 Clz 4 W + 7 Qtz + 4 Phl + 10 An = 4 Ms + 3 Mts + 2 Clz 2 W + 10 CO ₂ + 14 Clz + 21 Qtz + 12 Phl = 10 Cal + 12 Ms + 9 Mts 3 W + CO ₂ + 7 Qtz + 4 Phl + 7 An = Cal + 4 Ms + 3 Mts	525°C/.12 xCO ₂
BGR61 1) qtz-cal-pl-dol-clz-ms-bio-W-CO ₂ 2) K-Ca-Mg-Al-Si-O-H-C 3) qtz-an-cal-phl-dol-clz-ms-W-CO ₂	(P = 6kbar) 3 An + Cal + W = CO ₂ + 2 Clz Phl + 4 Clz + 6 CO ₂ = 2 W + 2 Qtz + Ms + 3 Dol + 5 An An + 2 Cal + Phl + 4 CO ₂ = 2 Qtz + Ms + 3 Dol 5 Cal + 3 Phl + 2 Clz + 13 CO ₂ = W + 6 Qtz + 3 Ms + 9 Dol	520°C/.14 xCO ₂

applied to BGR30) shows all possible equilibria among the endmembers of the phases making up the paragenesis. Phases and possible endmembers (limited to the ones available in the thermodynamic database) as well as the possible equilibria among these endmembers are listed separately for each sample in table 2. These diagrams primarily tell about frozen equilibrium P-T-X_{CO₂} conditions from the intersection of mutual equilibria. For the purpose of a metamorphic N-S profile in this work, information about real petrologic reactions, forming the frozen equilibria assemblages, is not needed.

Equilibrium P-T, T-X_{CO₂} or T conditions deduced from these diagrams are listed in table 2 and are discussed below.

DISCUSSION OF THE METAMORPHIC PROFILE

Table 2 and figure 6 show that mean PT conditions calculated for the Gotthard massif and the Nufenenzone are grouped nicely between 465 to 490 °C and 4800 to 5000 bar, independent of which chemical system was used for the P-T calculations. There is no obvious increase in T nor in P

Tab. 3 Microprobe analyses normalized following PETRAKAKIS (1985).

PLAGIOCLASE (formula based on 8 O)									
Sample	BGR2	BGR6	BGR17	BGR19	BGR30	BGR36	BGR39	BGR61	BGR73
SiO ₂	59.25	59.17	59.17	64.03	61.11	57.70	57.19	60.07	50.36
TiO ₂	0.00	0.02	0.03	0.00	0.00	0.01	0.01	0.00	0.00
Al ₂ O ₃	25.92	25.31	25.05	22.91	25.19	27.55	27.12	25.76	31.72
FeO	0.00	0.02	0.00	0.06	0.02	0.01	0.19	0.00	0.04
MgO	0.00	0.00	0.00	0.00	0.00	0.00	0.00	0.00	0.00
CaO	7.88	7.62	7.57	4.25	6.67	10.05	9.18	7.43	15.12
Na ₂ O	7.20	7.41	7.08	9.60	7.78	5.62	6.33	7.55	2.85
K ₂ O	0.02	0.06	0.08	0.04	0.01	0.05	0.06	0.07	0.02
Total	100.27	99.61	99.00	100.89	100.79	100.98	100.08	100.88	100.11
an	0.377	0.361	0.370	0.196	0.321	0.495	0.443	0.351	0.745
ab	0.622	0.635	0.626	0.802	0.678	0.502	0.553	0.645	0.254
or	0.001	0.004	0.005	0.002	0.000	0.003	0.004	0.004	0.001

CLINOZOISITE (Formula based on 25 O)								
Sample	BGR2	BGR6	BGR17	BGR30	BGR36	BGR55	BGR61	BGR73
SiO ₂	39.06	39.19	38.65	38.76	39.57	38.41	38.81	39.32
TiO ₂	0.12	0.14	0.11	0.07	0.17	0.08	0.12	0.13
Al ₂ O ₃	27.85	29.16	28.09	27.01	29.19	24.69	26.28	29.23
Cr ₂ O ₃	0.02	0.00	0.01	0.07	0.04	0.08	0.00	0.02
FeO	7.00	5.08	6.52	7.91	5.73	11.39	8.83	5.35
MnO	0.16	0.00	0.06	0.12	0.11	0.19	0.02	0.09
MgO	0.00	0.00	0.02	0.00	0.00	0.03	0.03	0.04
CaO	23.26	23.27	23.47	22.62	23.46	22.71	23.06	23.18
Total	97.47	96.84	96.92	96.55	98.28	97.58	97.15	97.36
zo	0.548	0.670	0.584	0.498	0.641	0.287	0.424	0.662
ep	0.452	0.330	0.416	0.502	0.359	0.713	0.576	0.338
pi	0.000	0.000	0.000	0.000	0.000	0.000	0.000	0.000

BIOTITE (Formula based on 11 O)									
Sample	BGR2	BGR6	BGR17	BGR19	BGR20	BGR36	BGR39	BGR61	BGR73
SiO ₂	37.38	36.35	36.64	36.36	36.89	36.59	36.56	37.70	36.67
TiO ₂	1.45	1.48	1.69	1.51	1.98	1.52	1.70	1.45	1.68
Al ₂ O ₃	18.11	18.48	17.86	17.93	15.99	18.45	18.08	17.16	18.30
Cr ₂ O ₃	0.07	0.18	0.01	0.00	0.01	0.17	0.10	0.00	0.10
FeO	17.32	20.15	18.57	20.22	17.78	19.10	19.04	15.01	16.91
MnO	0.08	0.04	0.05	0.04	0.11	0.07	0.05	0.01	0.10
MgO	11.61	8.76	10.65	9.44	12.49	10.04	9.93	13.82	11.09
CaO	0.00	0.01	0.00	0.00	0.01	0.06	0.00	0.00	0.01
Na ₂ O	0.12	0.13	0.15	0.12	0.17	0.07	0.10	0.11	0.06
K ₂ O	9.31	8.88	9.56	9.45	8.95	9.53	9.07	9.50	9.20
Total	95.47	94.44	95.18	95.07	94.37	95.60	94.65	94.75	94.14
xMg-Y	0.452	0.352	0.422	0.377	0.487	0.397	0.395	0.533	0.440
xFe-Y	0.378	0.454	0.412	0.453	0.388	0.424	0.425	0.325	0.376
xAl-Y	0.138	0.160	0.131	0.139	0.083	0.144	0.143	0.113	0.146
xTi-Y	0.028	0.030	0.034	0.030	0.039	0.030	0.034	0.028	0.034
xK-X	0.980	0.977	0.977	0.981	0.972	0.983	0.983	0.983	0.989

Tab. 3 (continued)

WHITE MICA (Formula based on 11 O)										
Sample	BGR2	BGR6	BGR17	BGR19	BGR30	BGR30	BGR36	BGR39	BGR61	BGR73
SiO ₂	46.63	46.89	47.35	46.92	46.81	46.24	47.09	47.65	47.82	47.37
TiO ₂	0.22	0.19	0.56	0.44	0.24	0.06	0.15	0.33	0.39	0.29
Al ₂ O ₃	34.16	34.87	33.50	34.37	35.15	40.26	34.24	33.63	32.40	33.49
Cr ₂ O ₃	0.08	0.06	0.00	0.00	0.04	0.02	0.02	0.09	0.00	0.07
FeO	1.73	1.29	1.54	1.34	1.30	0.41	1.92	1.41	1.94	1.33
MnO	0.03	0.00	0.00	0.00	0.01	0.00	0.01	0.02	0.00	0.02
MgO	0.72	0.68	1.49	1.07	0.64	0.11	0.67	0.96	1.71	0.94
CaO	0.04	0.00	0.00	0.00	0.00	0.82	0.00	0.00	0.00	0.06
Na ₂ O	0.50	0.69	1.16	0.89	1.72	6.44	0.56	0.68	0.57	0.54
K ₂ O	9.48	10.14	9.27	9.50	8.69	1.05	10.12	10.03	10.18	9.84
Total	93.58	94.81	94.87	94.52	94.61	95.40	94.79	94.80	95.01	93.95
xAl-Y	0.909	0.924	0.872	0.900	0.925	0.982	0.909	0.903	0.854	0.907
xNa-X	0.074	0.094	0.159	0.125	0.231	0.849	0.078	0.094	0.078	0.077
xK -X	0.923	0.906	0.841	0.875	0.768	0.091	0.922	0.906	0.922	0.918

GARNET (Formula based on 12 O)

Sample	BGR2	BGR6	BGR17	BGR19	BGR19	BGR30	BGR55	BGR73
SiO ₂	37.80	37.18	37.32	37.52	37.02	37.79	37.40	37.88
TiO ₂	0.16	0.09	0.18	0.03	0.02	0.12	0.13	0.10
Al ₂ O ₃	20.90	20.89	20.88	21.05	21.15	20.81	20.62	20.93
Cr ₂ O ₃	0.04	0.01	0.02	0.01	0.01	0.05	0.13	0.05
FeO	31.13	32.01	28.74	29.59	35.65	33.72	32.06	33.42
MnO	2.20	0.96	3.95	1.62	1.31	1.68	2.52	0.75
MgO	1.61	1.52	1.49	1.29	2.95	1.19	1.35	1.79
CaO	7.28	7.72	7.95	9.82	2.82	6.38	7.21	6.63
Total	101.11	100.39	100.52	100.93	100.92	101.74	101.42	101.55
alm	0.680	0.697	0.625	0.635	0.773	0.734	0.685	0.725
sps	0.049	0.022	0.089	0.036	0.029	0.038	0.057	0.017
pyr	0.064	0.061	0.059	0.051	0.117	0.047	0.053	0.071
grs	0.186	0.192	0.199	0.248	0.050	0.156	0.158	0.164

AMPHIBOLE (Formula based on 23 O)

CHLORITE (Formula based on 14 O)

Sample	BGR2	BGR36	BGR39	BGR36	BGR55	
SiO ₂	41.44	41.58	42.01	25.48	22.84	
TiO ₂	0.33	0.34	0.35	0.13	0.11	
Al ₂ O ₃	19.41	19.13	17.61	22.45	21.80	
Cr ₂ O ₃	0.04	0.05	0.08	0.02	0.08	
FeO	17.65	17.90	18.51	24.46	35.98	
MnO	0.11	0.16	0.14	0.09	0.10	
MgO	6.41	6.18	6.53	14.97	6.72	
CaO	10.32	10.72	10.28	0.00	0.21	
Na ₂ O	1.22	1.26	1.36	0.00	0.01	
K ₂ O	0.39	0.43	0.41	0.01	0.03	
Total	97.32	97.75	97.27	87.61	87.88	
Si	6.164	6.176	6.287	Xmg	0.522	0.250
Al ^{IV}	1.836	1.824	1.713			
Al ^{VI}	1.566	1.524	1.393			
Mg ^{VI}	1.421	1.369	1.457			
Fe ^{2+VI}	1.958	2.043	2.084			

from N to S. Moving to the Cornoschuppe and the Bedrettozone we again find that the mean results are internally homogeneous but here they lie between 515 to 525 °C and around 6000 bar. Thus there are two fairly uniform groups, separated by the Nufenenzone-Cornoschuppe contact. The only result that does not fit this pattern is BGR2 (530 °C in the Nufenenzone). BGR2 is a garnetiferous hornblende-garbenschiefer and might hold the same 520 °C fluid-T (at regional P 5000 bar) as similar rocks in the S of the contact rather than regional T.

Four possible limitations have to be considered when evaluating the tectonic consequences of the above findings:

(i) Applying the outlined technique for determination of metamorphic conditions does reduce the error to imprecisions of the electron microprobe data. Unfortunately the difference between conditions in the Helvetic units and the Penninic units is small and individual errors will possibly overlap. One way to make up for the insufficient precision in such cases, is to condense sampling and to choose several chemical rock systems. The former increases the resolution and reduces the possibility of incidental patterns, the latter helps to rule out systematic erroneous trends. The small scatter of the mean P-T groups, deduced with a very high sampling density (average: 1 sample/250 m) from various rock-chemistries, as well as the good correspondance with the data from KLAPER and BUCHER-NURMINEN (1987) seems to rule incident out.

(ii) More P-T estimates for Alpine Gotthard massif parageneses are needed to verify the two datapoints produced in this work (BGR17, 19). There is no proof (e.g. absolute age determination on metamorphic minerals used) for the assumption that the sampled shear zones have an Alpine paragenesis.

(iii) Thermodynamic data for tschermakite are of preliminary character (LIEBERMAN and KAMBER, 1991). Results for hornblende-garbenschiefer (BGR2, 36, 39) are based on diagrams calculated with Mts. There is a possibility that new thermodynamic end-member and mixing property data can result in minor changes in P-T for these rocks. Better data also for chl and cdt will hopefully enhance precision of P-T estimates in future.

(iv) There is a lack of good P-dependent reactions in most of the rocks from the Cornoschuppe and the Bedrettozone. Therefore mainly T-X_{CO₂} diagrams were used. P was set to 6.0 kbar indicated by BGR6. This assumption appears reasonable, since the resulting T-X_{CO₂} values are very closely grouped. The P-T diagrams have been calculated assuming pure water. This assumption is justified

by the presence of clz, which brakes down to form an, cal and water in the presence of CO₂.

In spite of these limitations, it is clear that the N to S increase in metamorphic conditions in the Cornopass area is of an abrupt character. This observation suggests that the Helvetic-Penninic tectonic contact in the Cornopass area was the locus of major metamorphic motion, lifting the southern units with respect to the northern ones. The abrupt increase in metamorphic conditions, mainly documented for T, is only preserved because the responsible motion along the Helvetic-Penninic boundary happened syn- to post-peak metamorphism.

This observation is fully compatible with a similar model for the Lukmanier area by RIDLEY (1989). In the downthrown block (Helvetic units in the Nufenen area) heating is predicted, and porphyroblast growth is late- and/or post-deformational as indicated by growth-deformation relations (Fig. 5a), whereas porphyroblasts in the upthrown blocks (Penninic units in the Nufenen area) tend to be pre- to syn-deformational (Fig. 5b). Vertical block movement can thus explain apparent diachroneity of deformation and metamorphism recorded by porphyroblast textures. The abundance of late- to post-D3 hornblende-garbenschiefer in practically all lithologies along the Helvetic-Penninic contact is striking. Ar-Ar dating of these minerals seems to offer an excellent opportunity to date at least one important episode of the postulated vertical block movement. Unfortunately no dates for the Nufenen area are available. One K-Ar date of hbl of the same type from Piora (STEIGER, 1964, sample S2) and Ar-Ar dates on hornblende-garbenschiefer from the Tauern Window, which are in a similar tectonic position (BLANCKENBURG and VILLA, 1988), are young (~25 Ma, ~21 Ma respectively). Dating of hbl from the Nufenen area will verify the indication of either a long duration or a late attainment of peak-metamorphic conditions in the area, as concluded by DEUTSCH and STEIGER (1985).

There is no way to expand these findings to the whole southern margin of GM until more reliable structural, petrologic and age data are available. The new results from the Nufenenpass area can only stress the importance of studying the locus of deformation and the change of the grade of metamorphism with time, in trying to understand the Lepontine "puzzle".

Conclusions

If we aim to understand the mechanisms for both metamorphism and tectonics for the present-day

geological settings along the southern border of the Gotthard massif we have to understand the mechanisms of transport and their timing in relation to metamorphism. The results of this work is a further step in this direction as they show some of the complications that can be encountered along the steeply dipping margin of the Gotthard massif. These complications can be summed up as follows:

(i) Metasediments from the Ultrahelvetice and the Northpenninic realm are very similar. Detailed mapping and lithostratigraphical correlation with well-known profiles (e.g. Joos, 1969) proved to be tools to get a better idea of the exact boundary in the Cornopass area. The recognition of the Cornoschuppe as a Penninic tectonic unit, possibly the Mesozoic cover of the Lebendun crystalline nappe, allowed for a new interpretation of the strong N-S metamorphic increase.

(ii) Detailed petrologic work can provide the resolution needed to study the character of N to S increase of P-T conditions. The use of equilibrium diagrams based on an internally consistent database have been shown to be very useful in this work. Much caution is needed in the interpretation of single thermo- or barometers because widely used minerals might be in disequilibrium with the peak-T paragenesis (e.g. "Quer"-biotite).

For the study area an abrupt increase in P and T at the Helvetic-Penninic boundary has been documented by means of careful petrologic work. This finding is explained in terms of syn- to post-peak metamorphic motion, lifting the southern units with respect to the northern ones, much the same as RIDLEY'S (1989) subvertical block movement model for the Lukmanier area.

(iii) Structural features for specific deformation phases (i.e. D2 or D3) do not have to be contemporaneous in different tectonic units. Late uplift can juxtapose different structural units, and this will probably displace Mesoalpine isogrades as shown for the Helvetic Nufenenzone and the Penninic Cornoschuppe in the Nufenenpass area. Still, comparing chemically similar strata, the possibility that different tectonic units went through different P-T-t histories provides another way to look for unit-boundaries, as characteristic metamorphic minerals can grow for example syn-deformational in one unit and post-deformational in the other. The comparison of garnets from Liassic graphitic schists in the Nufenenzone and Cornoschuppe is one example.

(iv) The abundance of hornblende-garbenschiefer along the Nufenenzone-Cornoschuppe contact is striking. Although they have a late, post-D3 paragenesis their equilibrium P-T conditions are indistinguishable from the Penninic

peak conditions in the area. Absolute age determinations on these rocks can pertain to the questions of timing and locus of metamorphism versus deformation.

Acknowledgements

This work is based on the author's diploma thesis. M. Engi is thanked for supervision and inspiring comments. G. Biino and I. Mercolli contributed with many fruitful discussions. M. Frei and N. Mancktelow carefully reviewed an earlier version of the manuscript. J.D. Kramers helpfully corrected the English. EMP analyses were made possible by SNF-credit 21-26579.89.

References

- ABRECHT, J., BIINO, G.G., MERCOLLI, I. and STILLE, P. (1991): Mafic-ultramafic associations in the Aar, Gotthard and Tavetsch massifs of the Helvetic domain in the Central Swiss Alps: markers of ophiolitic pre-Variscan sutures, reworked by polymetamorphic events? *Schweiz. Mineral. Petrogr. Mitt.*, 71, 295-300.
- BERMAN, R.G. (1988): Internally consistent data for minerals in the system Na₂O, K₂O, CaO, MgO, FeO, Fe₂O₃, Al₂O₃, SiO₂, TiO₂, H₂O, CO₂. *J. Petrology*, 29, 445-522.
- BERMAN, R.G. (1990): Mixing properties of Ca-Mg-Fe-Mn garnets. *Amer. Mineral.*, 75, 328-344.
- BERMAN, R.G., BROWN, T.H. and PERKINS, E.H. (1987): GEO-CALC, Software for calculation and display of pressure-temperature-composition phase diagrams. *Amer. Mineralogist*, 72, 861-882.
- BLANCKENBURG, F. v. and VILLA, I.M. (1988): Argon retentivity and argon excess in amphiboles from the garbenschists of the Western Tauern Window, Eastern Alps. *Contrib. Mineral. Petrol.*, 100, 1-11.
- CHATTERJEE, N.D. and FLUX, S. (1986): Thermodynamic Mixing Properties of Muscovite-Paragonite Crystalline Solutions at High Temperatures and Pressures, and their Geological Applications. *J. Petrology*, 27, 677-693.
- DEUTSCH, A. and STEIGER, R.H. (1985): Hornblende K-Ar ages and the climax of Tertiary metamorphism in the Lepontine Alps (south-central Switzerland): an old problem reassessed. *Earth Planet. Sci. Lett.*, 72, 175-189.
- EICHENBERGER, R. (1924): Geologisch-petrographische Untersuchungen am Südwestrand des Gotthardmassivs (Nufenengebiet). *Eclogae geol. Helv.*, 18, 451-483.
- EUGSTER, H.P., ALBEE, A.L., BENICE, A.E., THOMPSON, J.B. and WALDBAUM, D.R. (1972): The two phase region and excess mixing properties of paragonite-muscovite crystalline solutions. *J. Petrology*, 13, 147-179.
- FOX, J.S. (1975): Three-dimensional isograds from the Lukmanier Pass, Switzerland, and their tectonic significance. *Geol. Mag.*, 112, 547-564.
- FUHRMAN, M.L. and LINDSLEY, D.H. (1988): Ternary-feldspar modeling and thermometry. *Amer. Mineralogist*, 73, 201-215.

- HAFNER, S. (1958): Petrographie des südwestlichen Gotthardmassivs. Schweiz. Mineral. Petrogr. Mitt., 38, 123–256.
- HANSEN, J.W. (1972): Zur Geologie und Geochemie der Bündnerschiefererien zwischen Nufenenpass und Casata Toce. Schweiz. Mineral. Petrogr. Mitt., 52, 109–153.
- INDARES, A. and MARTIGNOLE, J. (1985): Biotite-garnet geothermometry in the granulite facies; the influence of Ti and Al in biotite. Amer. Mineralogist, 70, 272–278.
- JOOS, M.G. (1969): Zur Geologie und Petrographie der Monte-Giove-Gebirgsgruppe. Schweiz. Mineral. Petrogr. Mitt., 49, 277–323.
- KAMBER, B.S. and ENGI, M. (1992): Abstr. Annual Meeting of Schweiz. Mineral. Petrogr. Ges. 1992, Basel, Switzerland.
- KERRICK, D.M. and JACOBS, G.M. (1981): A modified Redlich-Kwong equation for H_2O , CO_2 and H_2O - CO_2 mixtures at elevated pressures and temperatures. Amer. J. Sci., 281, 735–767.
- KLAPER, E.M. (1986): Deformation und Metamorphose im Gebiet des Nufenenpasses, Lepontinische Alpen. Schweiz. Mineral. Petrogr. Mitt., 66, 115–128.
- KLAPER, E.M. and BUCHER-NURMINEN, K. (1987): Alpine metamorphism of pelitic schists in the Nufenen Pass area, Lepontine Alps. J. metamorphic Geol., 5, 175–194.
- KOHN, M.J. and SPEAR, F.S. (1990): Two new geobarometers for garnet amphibolites, with applications to southeastern Vermont. Amer. Mineralogist, 75, 89–96.
- KRETZ, R. (1983): Symbols for rock-forming minerals. Amer. Mineral., 68, 277–279.
- LEU, W. (1985): Geologie der Sedimentzüge zwischen Griessee und Passo del Corno (Nufenengebiet, Wallis). Eclogae geol. Helv., 78, 537–544.
- LIEBERMAN, J. and PETRAKAKIS, K. (1991): TWEEQU thermobarometry: analysis of uncertainties and applications to granulites from Western Alaska and Austria. Canadian Mineralogist, 29, 857–887.
- LIEBERMAN, J. and KAMBER, B.S. (1991): AGU Abstract, Fall Meeting, San Francisco 1991, pp. 564.
- LISZKAY, M. (1966): Geologie der Sedimentbedeckung des südwestlichen Gotthard-Massivs im Oberwallis. Eclogae geol. Helv., 58, 900–965.
- MILNES, A.G. (1974): The structure of the pennine zone: A new working hypothesis. Bull. Geol. Soc. Amer., 85, 1727–1732.
- OBERHOLZER, W. (1955): Geologie und Petrographie des westlichen Gotthardmassivs. Schweiz. Mineral. Petrogr. Mitt., 35, 320–410.
- PETRAKAKIS, K. (1985): MINSORT, a program for the processing and archivation of EMP analyses of silicate and oxide minerals. Neues Jahrbuch der Mineralogie, 8, 379–384.
- PROBST, P. (1980): Die Bündnerschiefer des nördlichen Penninikums zwischen Valser Tal und Passo di San Giacomo. Beiträge zur geologischen Karte der Schweiz, Druck Stämpfli & Cie AG.
- RAMSAY, J.G. (1979): Excursion in the area Nufenenpass-Griessee. Eclogae geol. Helv., 72, 299–304.
- RIDLEY, J. (1989), in *Evolution of metamorphic belts*, DALY et al., Eds (Geological Society Special Publication, 1989), pp. 103–115.
- STEIGER, R.H. (1964): Dating of Orogenic Phases in the Central Alps by K–Ar Ages of Hornblende. J. geophysical Res., 69, 5407–5421.

Manuscript received August 18, 1992; revised manuscript accepted April 4, 1993.

APPENDIX

SAMPLE DESCRIPTION

A brief petrographic description of the samples used for P-T estimations along the metamorphic profile is given here in a N to S order:

BGR17: *Garnetiferous clinozoisite bearing 2-mica gneiss (Gotthard massif):*

This rock was sampled from a presumably Alpine shear zone and shows a strong schistosity formed by bt, ms, qtz and partly recrystallized pl. Alpine recrystallization should have been strong enough to overprint possible older mineral chemistries. Czo cuts through the schistosity-forming minerals. Garnets are found as big (up to 2 cm in diameter) inclusion-rich (qtz, ilm, bt) porphyroblasts with thin less inclusion-rich rims as well as in form of very small (1–2 mm in diameter) inclusion-free grains. Detailed electron microprobe analysis on this rock showed that grt composition indeed monitors at least two different events as the cores of the big grts have a very different composition from the rims (see Tab. 3), which are chemically identical with the fine grained grt population and therefore believed to belong to the Alpine paragenesis³.

BGR19: *Garnetiferous 2-mica gneiss (Gotthard massif):*

Very similar to BGR17 but without czo. Bt is partly chloritized, but this may be caused by later retrogression and chl was therefore not used for peak-P-T estimation.

BGR73: *Graphitic garnetiferous 2-mica schist (Nufenen zone):*

In a very fine grained graphitic matrix of qtz, pl, ms, bt czo and ilm, undeformed, idiomorphic garnets (up to 1.5 cm in diameter) are the only porphyroblasts. Mrg, qtz and tur can be found as radially arranged inclusions as can be seen from figure 5. As mrg is absent in the matrix it was not used in the calculation.

EK178: *Chloritoid bearing garnetiferous 2-mica schist (Nufenen zone):*

For a description, see KLAPER and BUCHER-NURMINEN (1987). Published mineral chemistry allowed reconstruction of an equilibrium diagram between cld, grt, qtz, ms and bt.

BGR2: *Garnetiferous hornblende-garbenschiefer (Nufenen zone):*

This rock has been sampled 100 m N from contact with the Cornoschuppe. "garben" tex-

tured hbl, grt, czo and late bt cut through a the strong schistosity (D2) which is formed by well foliated ms and ilm and elongate pl and qtz. Bt has certainly grown significantly later than the other minerals. Growth of the other porphyroblasts is contemporaneous with the weak crenulation of the D2 foliation (D3). The whole paragenesis, except maybe for ms, is considered to monitor D3 P-T conditions.

BGR30: *Garnetiferous 2-white mica schist (Nufenen zone):*

A well foliated matrix of qtz, pl, ms and ilm is shot through with porphyroblasts of grt, 1 cm big flakes of pg and fresh czo. Pg and czo are found as inclusions in grt and therefore viewed as belonging to the peak-paragenesis.

BGR36: *Carbonatic hornblende-garbenschiefer (Cornoschuppe):*

"garben" textured hbl together with czo cut through a mm-layering of more carbonatic (cal, Fe-dol, qtz and pl) and more phyllitic layers (bt, ms, pl and late chl).

EK189: *Garnetiferous staurolite-bearing two-mica schist (Cornoschuppe):*

For a description, see KLAPER and BUCHER-NURMINEN (1987). The paragenesis reconstructed from published mineral chemistry is: grt-st-bt- czo -qtz.

BGR6: *Garnet-plagioclase-quartz fels (Cornoschuppe):*

Lenses of this rock, which is distinctive for the Lebendun sedimentary cover, are mainly built from grt (65%), pl (20%) and qtz (10%). Along the grain boundaries of these very coarse grained minerals bt, czo, mu and ilm can be found. Grt cores feature snowball-arranged qtz and ilm inclusions whereas the rims are inclusion-free.

BGR55: *Garnetiferous calcite-dolomite marble (Cornoschuppe):*

Along the polygonal carbonate-qtz grain boundaries skeletal grt, fresh chlorite and hypidiomorphic epidote can be found. Late clustered pg grows from triangle points and is not included in the peak-paragenesis.

BGR39: *Carbonatic hornblende-garbenschiefer (Bedrettozone):*

Very similar to BGR36 except for cal being the only carbonate phase (no Fe-dol).

BGR 61: *Clinozoisite bearing calcareous 2-micaschist (Bedrettozone):*

"Bündnerschiefer" s.s. characterized by layering of carbonatic parts (dol, qtz, pl) with phyllitic parts (ms, bt, pl). Granoblastic texture is indicated by big idiomorphic czo crystals which overgrow this layering.

³ The term "paragenesis" is used in its stricter sense, defining this part of a nowadays assemblage, in which all minerals were in equilibrium with each other at peak T.